JOURNAL OF OPTOELECTRONICS AND ADVANCED MATERIALS, Vol. 11, No. 11, November 2009, p. 1704 - 1712

Electro-optical characteristics of PIN photodiode under high thermal irradiated fields

ABD EL-NASER A. MOHAMED[a], MOHAMED M. EL-HALAWANY[a], HAZEM M. EL-HAGEEN[a,b*]
[a]*Electronics and Electrical Communication Engineering Department, Faculty Electronic Engineering,Menouf, 32951, Egypt*
[b]*Atomic Energy Authority, P.O. Box 29, Naser City, Cairo, Egypt*

In the present paper, they have analyzed deeply and parametrically the performance of PIN photodiodes employed in high temperature-irradiated environment. The radiation-induced photodiodes defects can modify the initial doping concentrations, creating generation-recombination centres and introducing trapping of signal charge carriers. Additionally, introduction rate of the lattice defects is thermally activated and decreases with increasing irradiation temperature as a result of annealing of the damage. The present work aims at a comparison of the behaviour of differently constructed Si and InGaAs PIN photodiodes after exposure to deferent conditions (ionizing gamma rays doses and electrons particles fluences respectively) of radiation with increasing temperature. Nonlinear relations are correlated to investigate the current-voltage and capacitance-voltage dependences based on the equivalent circuit of the PIN photodiodes where thermal and irradiation effects are considered. Thermal and irradiation effects are modelled and investigated over the practical ranges of interest. Both the ambient temperature and irradiation dose as well as the spectral power of incident light possess several effects on the electro-optical PIN photodiode characteristics (dark current, photocurrent, absorption coefficient, responsivity, quantum efficiency and directivity) and consequently SNR and BER for analog and digital optical link systems.

(Received July 29, 2009; accepted November 12, 2009)

Keywords: Radiation effects, PIN photodiode, Optoelectronics, Darckcurrent, Photocurrent

1. Introduction

Since several years, photonic technology is seriously considered for communication and monitoring applications in space-bone systems and nuclear projects. A major problem which arises when dealing with photonics in these environments is the presence of radiation fields. Space radiation includes mainly protons, electrons and heavy ions, whereas gamma and neuron radiation are a major concern around ground nuclear facilities. Two types of damage affect the electronic devices when they are exposed to the radiation [1, 2]. The first one is ionization damage, it generates electron–hole pairs along the path of the incident particle charged inside the semiconductor. It is a transitory damage because it disappears shortly after the particle strikes. In contrast, displacement damages cause alterations in the periodicity of the lattice, generating energy levels located in the forbidden band of the semiconductor. Such damage is considered permanent. The lattice defects affect the behavior of the semiconductor. For several reasons, interest in high-temperature electronics develops fast. If these components are to be used in a radiation environment, knowledge about the degradation under high-temperature irradiation conditions is highly desirable.

The current–voltage (I–V) technique is used to measure the space charge or carrier density in semiconductors [3–6]. Current measurements should therefore determine the rate of carrier creation and so the generation or the recombination rate. On the other hand, the capacitance–voltage (C–V) technique in reverse bias, measures the depletion region capacitance in p–n junctions and so is used to determine doping profiles within a semiconductor [7–9]. Measurements of the capacitance give information about fixed impurity states and defect centers in the band gap. This capacitance is associated with the bending of energy bands in the junction, and this is determined by the net ionized charge density.

Device testing, adequate system shielding and radiation tolerant design are some fundamental steps in the methodology that are needed to ensure the correct performance of electronics during system life. This methodology is called radiation hardness assurance [10, 11]. But, there is an increasing interest in the development of accurate modeling and simulation techniques to predict device response under different radiation conditions.

2. Physical basis

Radiation damage produces defects which can result in effects such as [12], Increased dark currents as defects act as centers of increase the generation bulk current; Degraded responsivity as defects act as electron or hole trapping centers for the photo generated pairs, resulting in an increased probability of recombination; Degraded rise and fall times due to de-trapping or a reduction in the carrier mobility. The increase in the dark current is expected to be the major change in thin junction devices such as photodiodes. The change in the device response and rise and fall times are expected to be small, but still require measuring. The increase in dark current can be related to the minority carrier lifetime of the semiconductor if the generation-recombination is dominated by mid-band levels caused by defects. Another source affecting the dark current

could be ionizing damage to the surface of the device, which would generally lead to a catastrophic rise in the current.

The defects may be primary defects, i.e. defects which originate directly from atomic displacements, or secondary defects resulting from the interaction of mobile primary defects with impurities. The first stage of the damage process is concluded when the PKA (primary knock-on atom) comes to rest. The vacancies and interstitials (known together as a Frenkel pair) produced will then diffuse through the semiconductor crystal until they form stable complexes. Many will recombine leading to an immediate repair of the lattice. However, some will combine to form stable defects such as di-vacancies, vacancy-impurity complexes, vacancy-dopant complexes, and larger clusters. These defects form effective recombination and trapping centers resulting in a decrease in the minority carrier lifetime, carrier density and carrier mobility. Defect centers position in the band gap determines their activity and hence the conduction mechanism in devices made from such material [13]. Deep traps are defects whose ionization energy, E, is much greater than k_BT (k_B is the Boltzmann constant and T is the temperature). They trap free carriers with the consequence that they reduce the conductivity considerably. In contrast, shallow traps are easily ionized at equilibrium since $\Delta E << k_BT$, and so they increase the conductivity by releasing trapped carriers. In depleted regions they contribute to the space charge and the voltage required for full depletion. Generation–recombination (g-r) centers are situated near the centre of the band gap, in which position their trapping for electrons and for holes is comparable, and so they easily generate or recombine (e–h) pairs. They can increase considerably the recombination of free carriers, which are removed to reduce the conductivity. However, more carriers are created at mid gap such that recombination also occurs at half band gap. Carrier densities then assume intrinsic values such that the Fermi level becomes pinned at midgap, the location for intrinsic behavior. The material becomes semi-insulating with low conductivity as a consequence. Defect centers can also act as compensation centers in the electrical neutral bulk of a semiconductor. Here, the deep levels are not easily ionized at equilibrium and have the effect of locking away free carriers to reduce the conductivity.

The initial response degradation [12] is probably related to type inversion of the low-doped layer from n- to p-type as a result of the incident radiation forming acceptor levels. At low integrated fluence, the acceptor state compensates the donor state until the effective doping concentration N_{eff} is reduced to that of the intrinsic semiconductor. On the other hand, at higher fluences, the effective doping is mainly provided by the radiation induced defects. The concentration of majority carriers decreases with the irradiation fluence as follows, $n = n_i - k_n\Phi$, where n_i is the initial carrier concentration, k_n is the rate of radiation-induced removal of carriers, and Φ is the radiation fluence. A semiconductor p–n junction acts as a capacitor. The depletion region capacitance of a uniformly doped lifetime diode at full depletion may be expressed in terms of the dielectric constants ε_0, ε_r. In this situation the effective carrier concentration is evaluated from:

$$N_{eff} = \frac{2C^2}{q\varepsilon_r\varepsilon_0 A^2}V \tag{1}$$

where A is the active diode area, q is the electronic charge and V is the full depletion voltage. This relation shows that $N_{eff} \alpha VC^2$, which may be simplified to $V \alpha C^{-2}$ for a constant effective carrier concentration, which is the case for uniform doping and is assumed for lifetime material. In any semiconductor, a rise in temperature will increase the current, since carriers become thermally activated to increase the effective carrier density, N_{eff}, so that the current $I \alpha N_{eff}$. An increase in light intensity is expected to have the same effect [13, 14]. Because the current is ohmic and is generated in the whole of the depletion region, the depletion width becomes a function of depletion voltage. The capacitance becomes a function of radiation and temperature since electrons and holes are thermally activated, and so N_{eff} is variable with radiation and temperature.

Photons that penetrate the semiconductor can be absorbed and its energy can be utilized in the generation of e–h pairs. The model that describes the rate of generation is [15]:

$$G_{opt}(x) = (1-r)\eta\frac{p_0\alpha}{h\nu}\exp(-\alpha x) \tag{2}$$

where r is the reflection coefficient, $(1-r)$ is the fraction of photons that penetrates the semiconductor, Previous reports in literature have stated that is independent of dose for 1 MeV electron irradiations up to 5×10^{15} cm^{-2} [16]. η is the quantum efficiency (the average number of electron–hole pairs created by each absorbed photon), P_0 is the incident light intensity at the semiconductor surface, h is the Planck constant, ν is the photon frequency, α is the absorption index and x is the depth variable. The optical spectral response of a PIN photodiode is called the optical sensitivity or the responsively of PIN photodiode and it is related to the total photon-induced current, which is the sum of the drift current in depletion layer as well as any diffusion current. If the width of the p-layer is much thinner than the inverse absorption coefficient, $1/\alpha$, the photon-induced current in the p-layer does not contribute to the total photon-induced current. The rate at which the electrical properties of the materials are degraded in a radiation environment is usually formulated in terms of the damage coefficient [3, 17, 18]. Usually, the analysis is based on the current–voltage characteristics, both in the dark and under illumination. These characteristics are highly sensitive to the radiation-induced changes of the minority carrier lifetime τ. In general, the damage coefficients for the mean minority carrier lifetime in semiconductors depend on the following parameters: type and energy of the incident particle, kind of material, types and concentration of impurities, injection level, temperature and elapsed time after irradiation.

In the present study, we have investigated a model of a PIN photodiode device with the maximum possible precision, in order to reproduce not only previous studies and experimental results reported, but also to be able to predict the behavior of the devices. The main objective of the present paper is using our model to estimate the electro-optical characteristics and consequently compare of the behavior of two differently constructed PIN photodiodes when they are irradiated by different dose/fluences of high-temperature gamma and electrons particles radiation.

3. Basic model, governing equations and analysis

3.1 Optical and electrical properties analysis

The dark current, I_D, for a device having depletion depth w, active area A and the effective carrier concentration, N_{eff} under high temperature irradiation T and radiation fluence Φ is given by [19, 20]:

$$I_D = \frac{qAw(T,\Phi)N_{eff}(T,\Phi)}{2\tau_r(T,\Phi)} \tag{3}$$

where τ_r is the minority carrier lifetime after irradiation and it is given by [12, 15, 20]:

$$1/\tau_r = 1/\tau_0 + K_r\Phi \tag{4}$$

where τ_0 denotes the pre-irradiation minority carrier lifetime, and K_r is the damage coefficient for τ_r. Assuming a linear relationship between damage increase and fluence, the damage coefficient for dark current K_D and light photocurrent K_P, can be defined by following equation [18]:

$$\Delta I_{D,P} = \left| I_{D,P}(\Phi) - I_{D,P}(0) \right| = K_{D,P}\Phi \tag{5}$$

A simple model of the annealing can be constructed if they assume that the radiation-induced defects anneal according to a first-order mechanism (exponential recovery) [21, 22], at a given absolute high temperature irradiation T, K_D can be related to an activation energy E by the Arrhenius formula:

$$K_D(T) = K_D(0)\exp(E/K_BT) \tag{6}$$

where K_B, is Boltzmann's constant.

Based on the data of [23-28], they carried out the following nonlinear thermal and radiation relations for the set of Si and InGaAs PIN photodiode, where they cast:

$$I_{D,P}(T,\Phi) = I_{D,P}(T)\times I_{D,P}(\Phi) \tag{7}$$

$$\left.\begin{aligned} I_{D_{SiPIN}} &= I_D(0) + 3.29\times10^{-24}\exp(831/T)\times\Phi \\ I_{P_{SiPIN}} &= I_P(0) - 7.8\times10^{-14}\begin{pmatrix} -1.137\times10^{-11}T^2 \\ +6.536\times10^{-9}T \\ +8.207\times10^{-8} \end{pmatrix}\times\Phi \end{aligned}\right\} \tag{8}$$

$$\left.\begin{aligned} I_{D_{InGaAsPIN}} &= I_D(0) + 5.5\times10^{-23}\exp(1876/T)\times\Phi \\ I_{P_{InGaAsPIN}} &= I_P(0) - 3.5\times10^{-22}\begin{pmatrix} -1.532\times10^{-7}T^2 \\ +4.231\times10^{-5}T \\ +0.07491 \end{pmatrix}\times\Phi \end{aligned}\right\} \tag{9}$$

Based on Eqn.1 and the results of [7-8] which shows the variation of the effective carrier concentration, N_{eff} of Si PIN photodiode with electron irradiation dose. They have cast the depletion layer capacitance with its initial value C_0, when a voltage V_{bias} is applied to a junction with the built-in potential ($V_{bi\ (Si)}$~0.65v [13] and $V_{bi\ (InGaAs)}$~0.3v [5]), under the form:

$$C(T,\Phi) = \frac{C_0\sqrt{\exp(-\beta\Phi)}}{a_1}\times\frac{(1+a_2T)}{\sqrt{|V_{bias}|+V_{bi}}} \tag{10}$$

where T is temperature, Φ is irradiation fluence, C_0/a_1=1.176×10^{-9}, a_2=0.001052,β=1.139×10^{-15} and V_{bias}=-1v.

The results of [5, 6] shows that there is no significant variation of the effective carrier concentration, N_{eff}, and C of InGaAs PIN photodiode with electron irradiation dose.

The optical absorption coefficient α of perfect semiconductor depends solely on the distribution of the electronic density of states [29]:

$$\alpha(h\nu) = \alpha_0(h\nu - E_g)^n \tag{11}$$

where α_0 is a factor with a specific value for a certain semiconductor, E_g is the bandgap energy, n=0.5 for InGaAs direct semiconductor and n=2 for Si indirect semiconductor. For imperfect semiconductor as aresult of radiation induced defects the energy band gab E_g is replace by Tauc bandgap energy E_{gTauc} [30], then α will became:

$$\alpha_{Tauc}(h\nu) = \alpha_0(h\nu - E_{g\,Tauc})^n \tag{12}$$

In this case the residual absorption near the bandgap due to the intraday is called the Urbach tail [31], and can be expressed with the following equation close to the bandgap:

$$\alpha_{Urb}(h\upsilon) = A_0\exp\left(\frac{\sigma}{K_BT}(h\upsilon - E_g)\right) \tag{13}$$

They need a function for α that is valid for the entire spectral range, i.e. an equation that combines Eqns. (12) and (13) and is smooth at E_{cross} [29]:

$$\alpha_{Tauc}(E_{cross}) = \alpha_{Urb}(E_{cross}) \quad (14)$$

$$\alpha'_{Tauc}(E_{cross}) = \alpha'_{Urb}(E_{cross}) \quad (15)$$

where α' denotes the first derivative with respect to the energy. With Equations (14) and (15) the following conditions are obtained:

$$E_{g_{Tauc}} = E_g - nE_{Urb}\left(1 + \ln\left(\left(\frac{\alpha_0}{A_0}\right)^{1/n}\left(\frac{1}{nE_{Urb}}\right)\right)\right) \quad (16)$$

where, $E_{Urb}(T) = E_{u0} \times T$

Table 1. Tauc and Urbach parameters of Si and InGaAs materials.

	Si[31, 32]	InGaAs[33, 34]
α_0	4685cm^{-1}	20000cm^{-1}
A_0	800cm^{-1}	5000cm^{-1}
E_{u0}	36 mev	9mev
n	2	0.5
E_g	$E_g = 1.166 - \frac{4.731\times10^{-4}T^2}{636+T}$	$E_g = \frac{0.812 - 3.26\times10^{-4}T}{+3.31\times10^{-7}T^2}$

The optical sensitivity, S, of a pin photodiode can be expressed as follow:

$$S(T,\Phi) = \frac{I_p}{P_0} = \frac{q\eta}{h\upsilon} \quad (17)$$

where the quantum efficiency, η, is given by:

$$\eta(T,\Phi) = \frac{I_p/q}{P_0(1-r)/h\nu} \quad (18)$$

The specific directivity is given:

$$D^*(T,\Phi) = \frac{\eta q\lambda}{hc\sqrt{2q(I_p+I_D)/A}} = S\sqrt{\frac{A}{2q(I_p+I_D)}} \quad (19)$$

3.1 Analog and digital receiver performance analysis

The equivalent circuit of simple model of a photodetector receiver shown in Fig.1 is considered to develop the performance of the device under consideration.

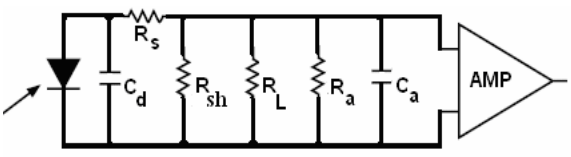

Fig. 1. The equivalent circuit a photodetector receiver.

The potheyr signal-to-noise ratio *S/N* at the output of an analog optical receiver is defined by [35]:

$$S/N = \frac{<I_p^2>}{<I_{nT}^2>} = \frac{<I_p^2>}{<I_Q^2>+<I_D^2>+<I_T^2>+<I_{amp}^2>} \quad (20)$$

where $<I_p^2> = 0.5m^2I_p^2$, *is signal power,*

$0.25 < m$ (*analog modulation index*) < 0.5,

$<I_Q^2> = 2qBI_p$, *is the quantum noise,*

$<I_D^2> = 2qBI_D$, *is dark current noise,*

$<I_T^2> = 4KBT/R_L$, *is thermal noise current , and*

$<I_{amp}^2>$, is the total noise associated with amplifier, it is referred to thermal noise of load resistor R_L by the amplifier noise figure F_n.

With this assumption, the analog Signal to Noise ratio S/N is:

$$S/N = <I_p^2>/(2qB(I_p+I_D) + 4KTBF_n/R_L) \quad (21)$$

where $B=1/2\pi R_TC = 1/3t_r$ is bandwidth and t_r is rise time.

For practical purpose, R_s is much smaller than the load resistance R_L and can be neglected. Also R_a is much large than the load resistance R_L, so they can suppose that:

$R_T = R_S + (R_L//R_{sh}// R_a)$, $R_T \approx R_L$ *and* $C \approx C_d // C_a$.

A number of different field-effect transistors can be used for front-end digital receiver designs [35]. In this case the total mean-square noise is modified as:

$$<I_{nT}^2> = A^2(2qBi_2 <i_p> + q^2B^2\delta) \quad (22)$$

where δ is a dimensionless parameter characterizing the thermal noise of receiver.

$$\delta = \frac{i_2}{q^2B}\left(2qI_{gate} + \frac{4KT}{R_b} + \frac{4KT\Gamma}{g_mR_b^2}\right) + \left(\frac{2\pi C}{q}\right)^2\frac{4KT\Gamma}{g_m}i_3B \quad (23)$$

For gigabit-per-second data rates, for example, the lotheyst-noise receivers are made using GaAs metal semiconductor field-effect transistors preamplifiers. The typical values of GaAs MESFET parameters are $C \approx C_d // C_a // C_{gd} // C_{gs}$, C_{gd}=0.01-0.05pF, C_{gs}=0.2-0.5pF, g_m=15-50mS, the numerical constant r = 1.1-1.75, I_{gate}=1-1000nA and the detector bias resistor $R_b = 10^5\Omega$. Let us consider the special case when Gaussian input pulse shape *h(t)* with the spread parameter Δ=0.1 given by Eqn. 24, $value_{off} = 0$ and for a raise cosine output, the values of i_2 and i_3 are 0.383 and 0.025 [35].

$$h(t) = \frac{b_{on}}{\sqrt{2\pi}\Delta T_b}e^{(-t^2/2\Delta^2T_b^2)} \quad (24)$$

The worst case of shot noise in any particular time slot occurs when all neighboring pulses are 1, since this case causes the greatest amount of intersymbol interference.

Under this conditions, the mean unity gain photocurrent = 1 over a bit time T_b for a 1 pulse and for a 0 pulse (with all adjacent pulses being 1) are:

$$< i_p >_1 = \frac{\eta q b_{on}}{h\nu T_b} \int_{-\infty}^{\infty} h(t)dt \cong \frac{\eta q b_{on}}{h\nu T_b} , \quad (25)$$

$$< i_p >_0 = \frac{\eta q b_{on}}{h\nu T_b} (1-\zeta) \quad (26)$$

The factor $(1-\zeta)$ is thus the fractional energy of a pulse 1 that has spread outside of its bit period as it traveled through the optical fiber, in the case of $\Delta = 0.1$, $\zeta \sim 1$.

In this case the Bit Error Rate (BER) can be expressed as:

$$BER = 0.5\left(1 - erf\left(0.345(S/N)\right)\right) \quad (27)$$

4. Results and discussion

Based on the above model, electro-optical characteristics of two different types Si and InGaAs PIN photodiode are processed in high temperature electron particles and gamma rays irradiations fields. The double impact of thermal and radiation effects are analyzed over wide ranges of causes (affecting parameters). As $10^{12} > \Phi$, Fluence, e/cm^2<10^{16} and $300 > T$, Temperature, K<500. Special software programs are designed, cast and employed to handle the given basic model, where variation of set of electrical and optical devices parameters $\{I_D, I_P, \alpha, \eta, S\}$ against variations of a set of two effects $\{T, \Phi\}$ are processed. The devices parameters are computed on bases of results of [23-28]. These variations will effect on response time and responsivity of the devices. Then they estimate the high temperature irradiation induced change of SNR and BER of devices for analog and digital applications. Samples of the obtained results are displays in Fig. 2-11, for the processed Si and InGaAs devices of optical wavelengths of λ=950 nm and 1550 nm respectively.

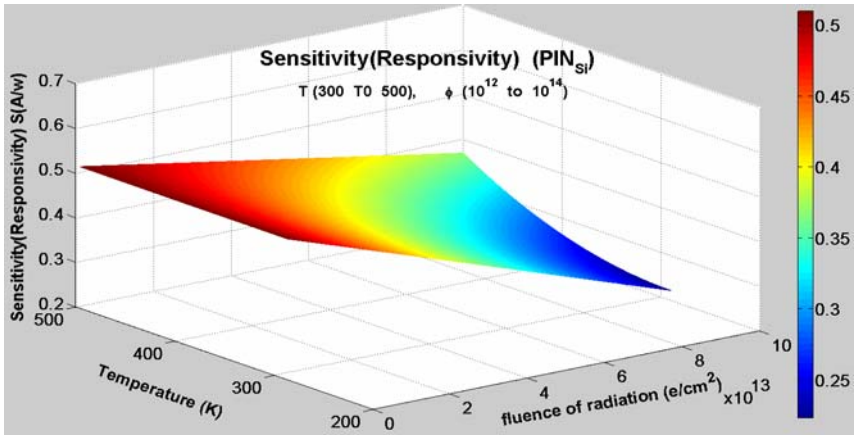

Fig. 2. Sensitivity of irradiated Si PIN photodiode at various radiation fluence and temperature.

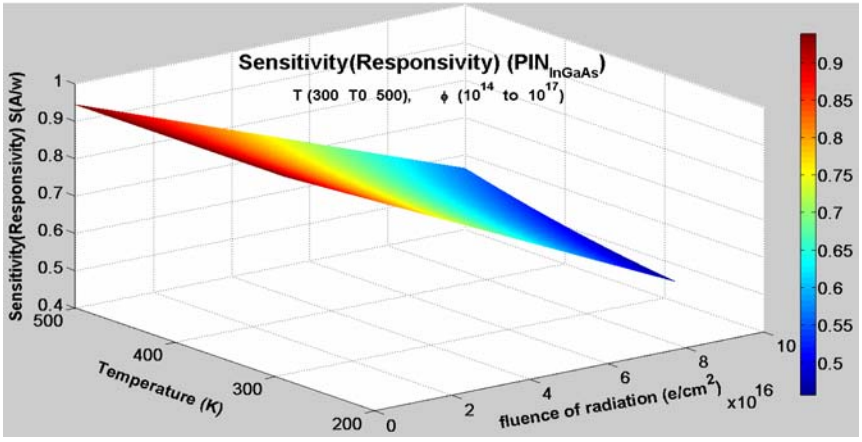

Fig. 3. Sensitivity of irradiated InGaAs PIN photodiode at various radiation fluence and temperature.

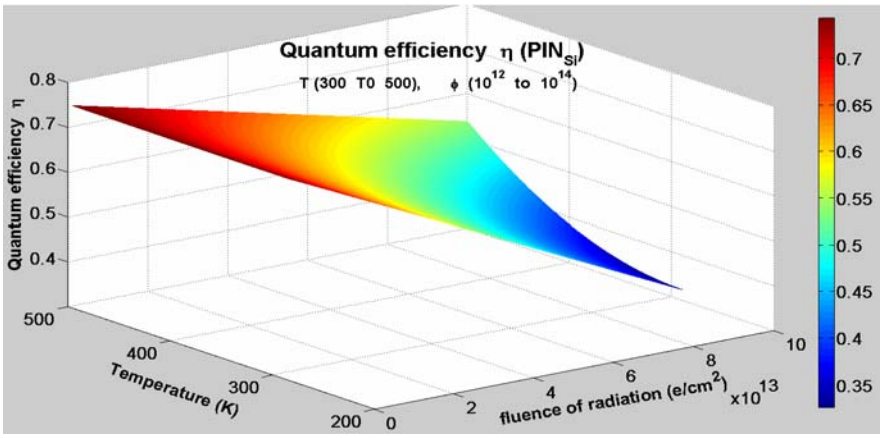

Fig.4. Quantum efficiency of Si PIN photodiode at various radiation fluence and temperature.

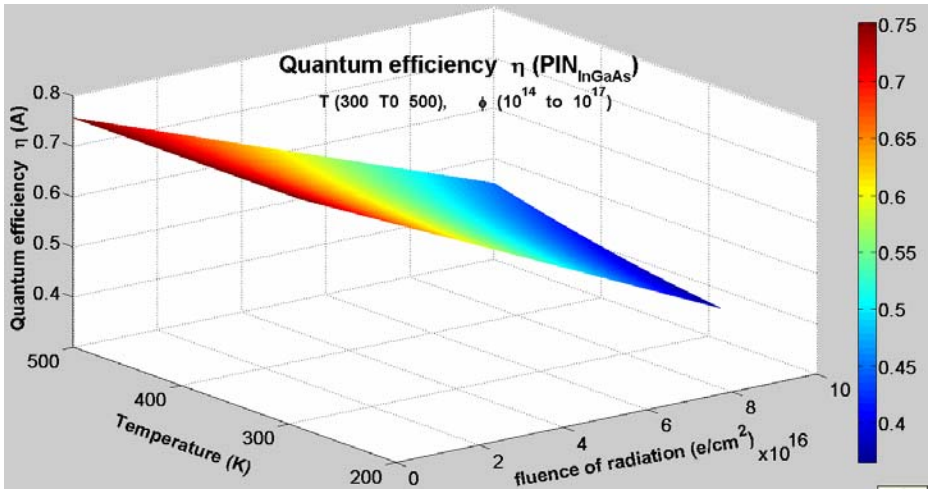

Fig.5. Quantum efficiency of InGaAs PIN photodiode at various radiation fluence and temperature.

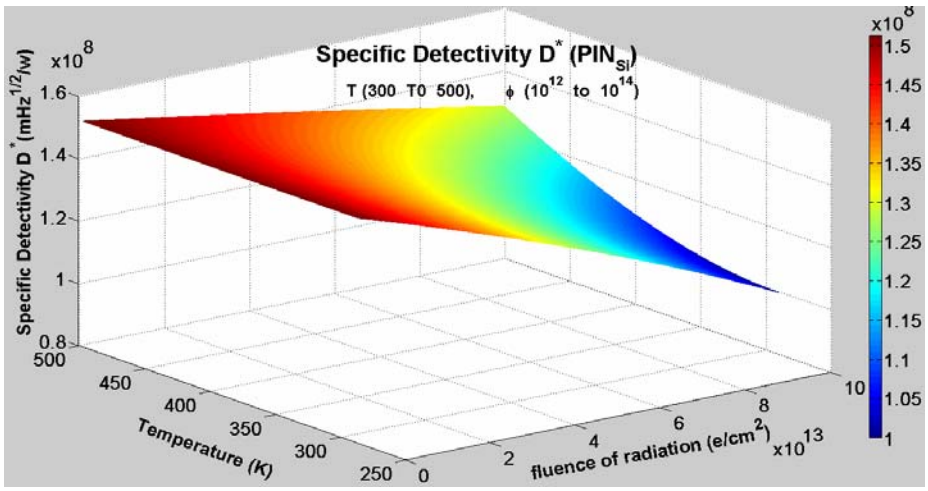

Fig. 6. Variation of specific detectivity of Si PIN photodiode versus radiation fluence and temperature.

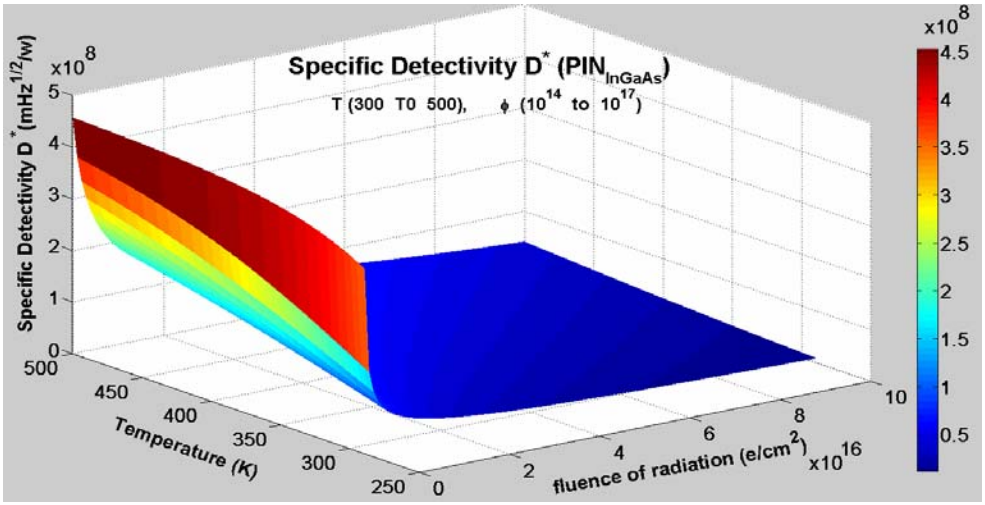

Fig. 7. Variation of specific detectivity of InGaAs PIN photodiode at various radiation fluence and temperature.

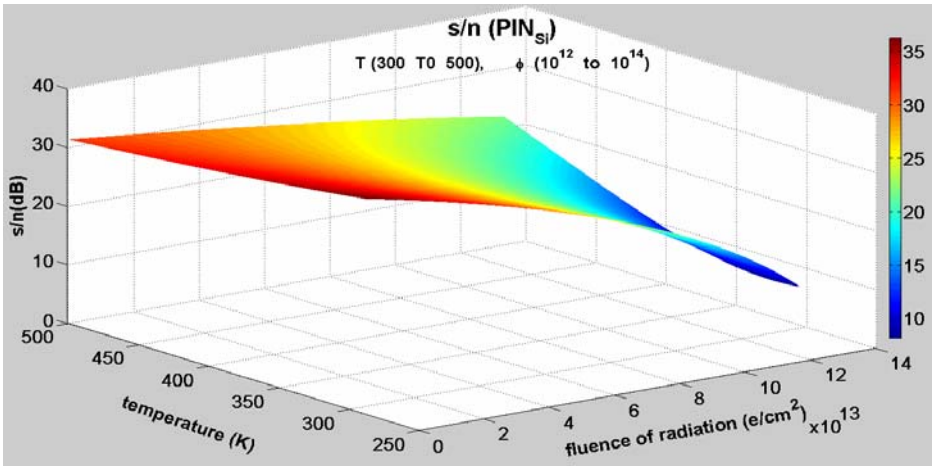

Fig. 8. Plot of s/n of Si PIN photodiode versus radiation fluence and temperature, m=0.3, F_n=3dB, R_L=100Ω.

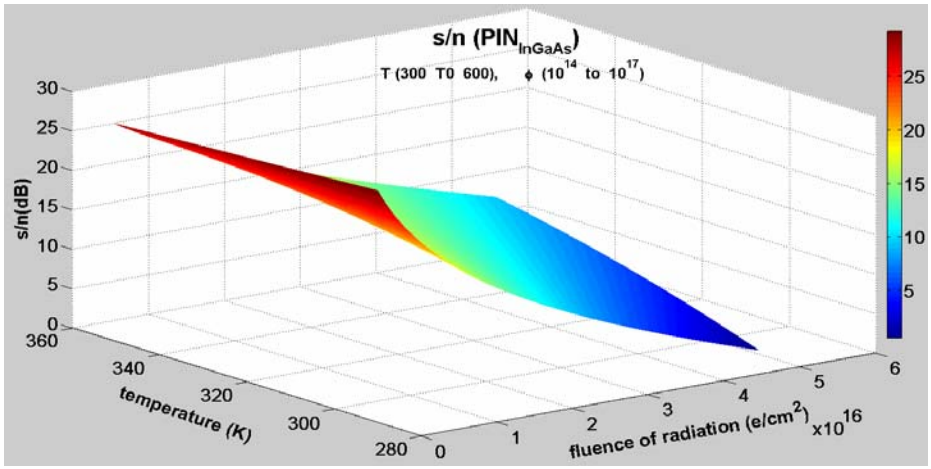

Fig. 9. Plot of s/n of InGaAs photodiode versus radiation fluence and temperature, m=0.3, F_n=3dB, R_L=500Ω.

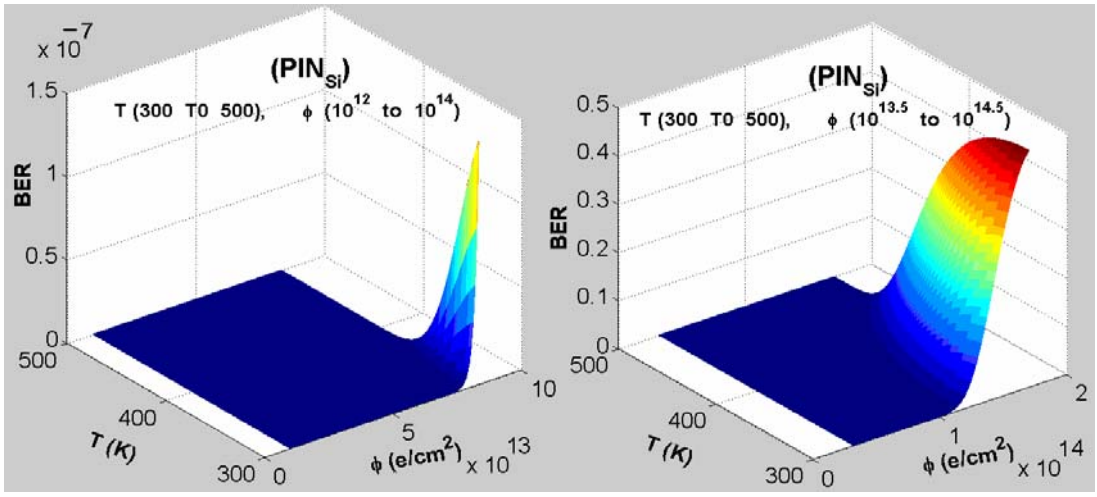

Fig. 10. Plot of BER Si photodiode versus radiation fluence and temperature.

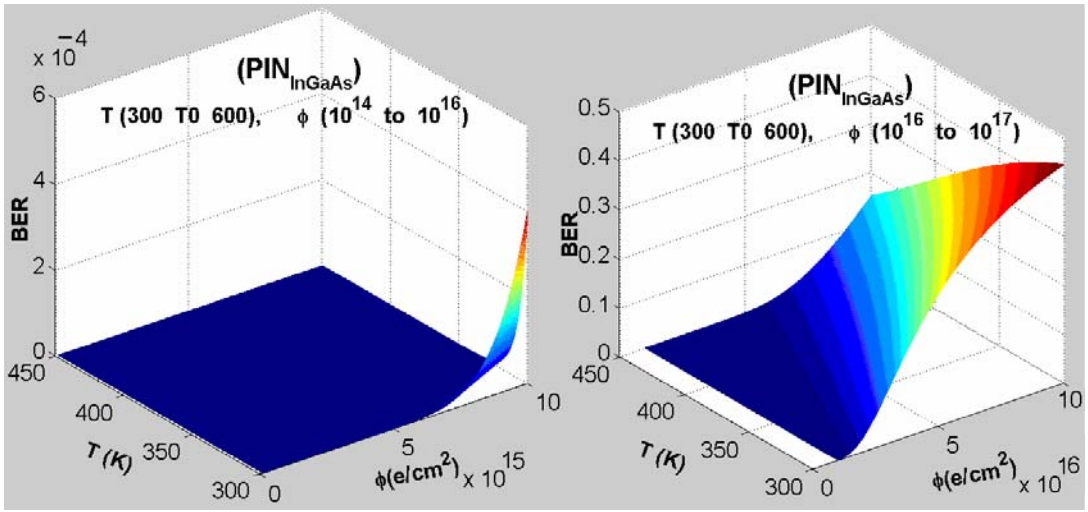

Fig. 11. Plot of BER InGaAs photodiode versus radiation fluence and temperature.

These figures assure the following:

i) The damage caused by fluence Φ, decrease I_P, η and S and increases I_D whatever the set of effect T.

ii) The value of the absorption coefficient at a particular energy in the absorption edge region was found to increase with the increase of the irradiation dose.

iii) The annealing caused by temperature T, decrease slightly the negative effects of irradiation on device performance.

iv) The device is more stable at higher optical power incident for all devices types and for all the set of effects {T, Φ}.

v) The Si PIN photodiode appear to be the most sensitivity to irradiation, the drop of I_P for a given decade of gamma fluence is large in Si than in InGaAs at the equivalent electron radiation of this gamma fluence.

vi) By studying SNR and BER for analog and digital applications, it is found that the devices are not reliability if device employed in gamma fluence above 10^{14} e/cm^2 or electrons fluence above 10^{17} e/cm^2.

5. Conclusions

The response of different types of PIN photodiode optical detector in different conditions of high temperature irradiation is modeled and investigated under wide ranges of affecting parameters. The following conclusions are clarified

1- Radiation damage produce photodiodes defects, these defects can modify the initial doping concentrations, creating g-r centers and introducing trapping levels. These modifications are mainly responsible for the degradation of device in high temperature irradiation.

2- Increasing of the absorption coefficient at a particular energy with increase of the irradiation dose is supposed to be connected with bond rearrangements and atomic disorder in the investigated amorphous composition.

3- The degradation of device performance and the introduction rate of lattice defects decrease with increasing irradiation temperature. This result suggests that creation

and recovery of the radiation damage proceeds simultaneously at high temperature.

4- Systematic studies (for a review, see Ref. [36-39]) by deep level transient spectroscopy (DLTS) performed in Si and InGaAs devices have shown that, the defects induced by radiation are primary defects in InGaAs such as the vacancies and interstitials, thermally stable at 300 K. But in Si, they are secondary defects resulting from the interaction of the primary defects with impurities such as the A center (complex vacancy –oxygen pair) and E center (complex vacancy –phosphorous pair) or with each others such as deviancies. This is the suggested reason for making InGaAs PIN photodiode is more radiation hardness than Si PIN photodiode.

References

[1] Y. K. Akimov, Instruments and Experimental Techniques **50**(1), 1 (2007).
[2] J. R. Srour, et al., IEEE Trans. on Nucl. Sci. **50**(3) (2003).
[3] S. Onoda, et al., Radiation Physics and Chemistry **60**, 377 (2001).
[4] A. M. Saad, J. Phys. **80**, 1591 (2002).
[5] G. J. Shaw, et al., Appl. Phys. **74**(3), 1629 (1993).
[6] G. J. Shaw, et al., Appl. Phys. **73**(11), 7244 (1993).
[7] S. Krishnan, G. Sanjeev, M Pattabi, Nucl. Instr. and Meth. in Physics Research **B264**, 79 (2007).
[8] M. Pattabi, S. Krishnan, G. Sanjeev, Solar Energy Materials and Solar Cells **91**, 1521 (2007).
[9] A. Simon, et al., Nucl. Instr. and Meth. in Physics Research B **260**, 304 (2007).
[10] M. Van Uffelen, I. Genchev, F. Berghmans, SPIE Proceeding **5465**, (2004).
[11] K. Gill, et al., submitted for presentation at the RADECS Workshop, Madrid, Spain, Sept. 2004.
[12] D. Dotheyll, et al., Nucl. Instr. and Meth. in Physics Research A **424**, 483 (1999).
[13] M. McPherson, J. Opt. A: Pure Appl. Opt. **7**, S325 (2005).
[14] M. McPherson, Semicond. Sci. Technol. **12**, 1187 (1997).
[15] M. A Cappelletti, et al., Semicond. Sci. Technol. **21**, 346 (2006).
[16] S. Onoda, et al., IEEE Trans. on Nucl. Sci. **49**(3), 1446 (2002).
[17] B. Danilchenko, et al., Solar Energy Materials & Solar Cells **92**, 1336 (2008).
[18] H. Ohyama, et al., Appl. Phys. Lett. **82**(2), 296 (2003).
[19] M. A Cappelletti, et al., Semicond. Sci. Technol. **23**, 025007 (2008).
[20] M. Mbarki, G. C. Sun, J. C. Bourgoin, Semicond. Sci. Technol. **19**, 1081 (2004).
[21] J. R. Srour, Fellow, D. H. Lo, IEEE Trans. on Nucl. Sci. **47**(6), 2451 (2000).
[22] M. Moll, E. Fretwurst, G. Lindstrom, Nucl. Instr. and Meth. in Physics Research **426**, 87 (1999).
[23] H. Ohyama, et al., Nucl. Instr. and Meth. in Physics Research B **219–220**, 718 (2004).
[24] H. Ohyama, et al., Physica B **340–342**, 337 (2003).
[25] K. Takakuraa, et al., Physica **B 376–377**, 403 (2006).
[26] H Ohyama, et al., Semicond. Sci. Technol. **11**, 1461 Printed in the UK (1996).
[27] H. Ohyama, et al., Physica B **308–310**, 1226 (2001).
[28] H. Ohyama; et al., Physica E **16**, 533 (2003).
[29] Raoul Schroeder, Charactrization of Organic and Inorganic Optoelectronic Semiconductor Devices Using Advanced Spectroscopic Methods, Doctor of Philosphy in Physics, Faculty of the Virginia Polytechnic Institute and State University, 2001.
[30] J. Tauc, Amorphous and liquid semiconductors, New York: Plenum Press, 1974.
[31] Y. Pan, F. Inam, M. Zhang, D. A. Drabold, J. Physical Review Letters **100** (206403), 1 (2008).
[32] M. A. Green, Solar Energy Materials & Solar Cells **92**, 1305 (2008).
[33] J.H. Wolter, G. D. Khoe, J. E. M. Haverkort, Polarization independent Interferometric Switches Based on III/V Quantum Well, Bastiaan Hendrik Peter Dorren, Eindhoven, 1999.
[34] S. Adachi, Physical properties of III-V Semiconductor compounds InP, InAs, GaAs,GaP, InGaAs, and InGaAsP, John Wiley & Sons, Inc., USA, 1992.
[35] G. E. Keiser, Optical Fiber Communications, McGraw-Hill, 3rd Ed., NY, USA, 2000.
[36] T. Kudou, et al., J. Radioanalytical & Nucl. Chem. **239**(2), 361(1999).
[37] J. C. Bourgoin, Solar Energy Materials & Solar Cells **66**, 467 (2001).
[38] J. C. Bourgoin, M. Zazoui, Semicond. Sci. Technol. **17**, 453 (2002).
[39] I. Pintilie, et al., Physica B **340–342,** 578 (2003).

*Corresponding author: hazemhageen@hotmail.com